RP105 exerts hepatoprotective effects in sepsis by modulating the SOCS2/JAK2/STAT3 signaling pathway

QIN DENG[1*], HONG DUO[2,3*], QIFA YE[2,3*], RUOPING CHEN[1], ZHIHUI FU[1], JIANSHENG XIAO[1], HUAQIN PAN[2-4] and QI XIAO[1]

[1]Department of Transplantation, The First Affiliated Hospital, Jiangxi Medical College, Nanchang University, Nanchang, Jiangxi 330006, P.R. China; [2]Hubei Key Laboratory of Medical Technology on Transplantation, Wuhan, Hubei 430071, P.R. China; [3]Zhongnan Hospital of Wuhan University, Institute of Hepatobiliary Diseases of Wuhan University, Transplant Center of Wuhan University, Transplant Intensive Care Unit, Wuhan, Hubei 430071, P.R. China; [4]Department of Critical Care Medicine, Zhongnan Hospital of Wuhan University, Clinical Research Center of Hubei Critical Care Medicine, Wuhan, Hubei 430071, P.R. China

Received July 8, 2025; Accepted September 2, 2025

DOI: 10.3892/ijmm.2025.5666

Abstract. Sepsis-induced liver injury increases mortality through inflammatory dysregulation. Although Radioprotective 105 (RP105) modulates inflammation, its role in septic liver injury remains unclear. The present study investigates the mechanism of RP105 in sepsis-driven hepatic damage. Sepsis was induced in RP105 knockout (KO) and wild-type (WT) mice via cecal ligation and puncture (CLP). Liver injury was assessed by serum alanine aminotransferase (ALT)/aspartate aminotransferase (AST), histology (H&E), inflammatory markers (anti-myeloperoxidase, F4/80, IL-1β, IL-6 and TNF-α) and apoptosis markers (Caspase-3, BAX/BCL-2 ratio, GADD45A and PUMA). RNA sequencing identified key differentially expressed genes. RP105-suppressor of cytokine signaling (SOCS) 2 interaction was validated by co-immunoprecipitation (Co-IP) and JAK2/STAT3 pathway activity was measured by western blotting. Lipopolysaccharide-stimulated RP105-KO macrophages were used *in vitro*. RP105-KO mice exhibited exacerbated liver injury post-CLP, evidenced by significantly elevated ALT/AST (P<0.001), expanded hepatic necrosis (P<0.001), increased inflammatory infiltration (P<0.001), upregulated pro-inflammatory cytokines (IL-1β, IL-6 and TNF-α; P<0.001) and enhanced Caspase-3 expression (P<0.001). RNA-seq identified SOCS2 as a key RP105-regulated DEG (fold change >2.0; FDR <0.05). Co-IP confirmed RP105-SOCS2 binding in WT liver which was absent in KO mice. SOCS2 protein remained decreased in KO + CLP vs. WT (P<0.001). RP105 deletion activated JAK2/STAT3 signaling *in vivo* and *in vitro* (P<0.001). RP105 protects against septic liver injury by binding SOCS2 to inhibit JAK2/STAT3 signaling, thereby attenuating inflammation and apoptosis. The present study is the first to demonstrate the RP105-SOCS2 interaction in septic liver injury, revealing the RP105/SOCS2 axis as a potential therapeutic target.

Correspondence to: Dr Qi Xiao, Department of Transplantation, The First Affiliated Hospital, Jiangxi Medical College, Nanchang University, 17 Yongwai Zheng Jie Street, Nanchang, Jiangxi 330006, P.R. China
E-mail: ndyfy05705@ncu.edu.cn

Dr Huaqin Pan, Zhongnan Hospital of Wuhan University, Institute of Hepatobiliary Diseases of Wuhan University, Transplant Center of Wuhan University, Transplant Intensive Care Unit, 169 Donghu Road Wuchang, Wuhan, Hubei 430071, P.R. China
E-mail: phq2012@whu.edu.cn

*Contributed equally

Key words: sepsis, liver injury, radioprotective 105, suppressor of cytokine signaling 2

Introduction

Sepsis is defined as a life-threatening systemic inflammatory response syndrome caused by a dysregulated host response to infection, contributing to a considerable global mortality rate (as of 2017, ~48.9 million cases of sepsis were recorded globally, with 11 million reported sepsis-related mortalities, accounting for 19.7% of all global mortalities) (1). The initial event of sepsis is the recognition of microbe-derived pathogen-associated molecular patterns or endogenous damage-associated molecular patterns by host pattern recognition receptors (2). This recognition triggers intracellular signal transduction pathways. Under physiological conditions, immune cells interact via this signaling network, inducing an innate immune response to eliminate pathogens and maintain cellular stability. However, certain host signaling pathways in sepsis become abnormally activated, leading to an explosive release of cytokines and alarmins (3). These inflammatory mediators markedly upregulate the expression of inflammation-related genes and act as key effector molecules in driving excessive systemic inflammatory responses and subsequent immunosuppression. This process further promotes the massive release of inflammatory mediators such as cytokines and chemokines, ultimately culminating in a cytokine storm (4,5).

The liver carries out a key role as a defensive barrier that protects the body against potential threats (6). It can be activated by microbes or alarm signals, resulting in the release of pro-inflammatory cytokines and the recruitment of immune cells to assist in microbial clearance. Additionally, the intricate immune surveillance mechanisms of the liver, supported by its strategic anatomical positioning, enable it to collaborate with both parenchymal and non-parenchymal cells to eliminate bacteria from the bloodstream and regulate the inflammatory and immune responses. This collaboration mitigates the risk of bacteremia and serves as a notable barrier against microbial invasion (7). However, the liver is frequently targeted by dysregulation of inflammation. Immune cells are susceptible to various substances. These substances include antigens, endotoxins, danger signals and microorganisms circulating in the bloodstream. Excessive stimulation may cause these cells to become abnormally activated and may also make them undergo apoptosis which disrupts immune function and contributes to inflammation dysregulation (8,9). Therefore, prompt intervention targeting liver injury during sepsis management is key to effectively mitigating inflammatory responses and cytokine storms, thereby protecting against further organ damage and improving patient outcomes.

Radioprotective 105 (RP105), also known as CD180, is a type I transmembrane protein characterized by an extracellular domain rich in leucine-rich repeats (LRRs) and a short cytoplasmic tail (10). Analogous to the Toll protein in Drosophila, RP105 was the first mammalian molecule to exhibit similarity to Toll through its extracellular LRRs. Lipopolysaccharide (LPS) is the primary component of the cell wall of gram-negative bacteria. It is also a key virulence factor. It causes infections such as sepsis and septic shock. During sepsis progression, LPS binds directly to pattern recognition receptors on immune cell surfaces. This binding activates the Toll-like Receptor 4 (TLR4) inflammatory signaling pathway. This activation triggers a release of inflammatory cytokines, resulting in an 'inflammatory cytokine storm' that can damage tissues and organs. As a key negative regulator of the TLR4 signaling pathway and an essential modulator of the immune system (11,12), RP105 prevents the excessive production of pro-inflammatory cytokines by inhibiting TLR4 mediated pro-inflammatory signals, serving as a protective strategy against exaggerated inflammatory responses. Consequently, RP105 carries out a key role in regulating immune response and controlling inflammation during sepsis.

Although numerous studies have reported the anti-inflammatory effects of RP105 in various disease models (13-16), its effect on sepsis-induced liver injury remains poorly documented. Moreover, the molecular mechanisms underlying the protective role of RP105, particularly whether it modulates intracellular cytokine signaling pathways, have not been elucidated. Therefore, the present study aimed to investigate the function of RP105 in sepsis-induced hepatic injury using a CLP mouse model.

Materials and methods

Mice and treatments. Wild-type (WT) mice and RP105 knockout (KO) mice [total number, 24 (WT, 12; KO, 12); male C57BL/6 mice; 8-12 weeks old; weighing 20-25 g] were purchased from GemPharmatech Co. Ltd. After purchase, the mice were raised at the Animal Experiment Center of Zhongnan Hospital of Wuhan University (Wuhan, China). Mice were kept in a breeding environment with a room temperature of 20-25˚C, humidity 50-70% and a 12:12 h light-dark cycle. All mice had free access to standard animal food and water. All experimental procedures were conducted in accordance with the National Institutes of Health Guidelines for the Care and Use of Laboratory Animals (17). Every effort was made to minimize the suffering of the mice used. Before the official experiment begins, the mice undergo an adaptive feeding period and are provided with sterilized clean drinking water. Genotypes of the knockout mice were confirmed using PCR. WT and KO mice were randomly assigned to different treatment groups (n=6 for single-variable animal experiments following previous studies that also used six animals per group to ensure reproducibility and statistical reliability) (18,19), data collection and analysis was carried out under blinded conditions.

Anesthesia protocol. C57BL/6 mice were anesthetized by inhalation of 5% isoflurane for induction, followed by maintenance with 2-2.5% isoflurane. The animals were positioned in a prone position on a 37˚C thermoregulated heating pad (Harvard Apparatus) with continuous monitoring of rectal temperature maintained at 36.5±0.5˚C.

Animal procedures. In this experiment, the duration of the laparotomy procedure for cecal ligation and puncture (CLP) is 10 min; the modeling cycle of the CLP model (the time from the completion of the modeling procedure to the end of the experiment) is 24 h. Following anesthesia, a 1 cm midline laparotomy was carried out on the left side of the xiphoid to expose the cecum. The cecum was then ligated at 75% of the distance between the distal pole and the base using 4-0 silk suture, followed by two through-and-through punctures with a 25-gauge needle near the distal end. The cecum was subsequently repositioned and the abdominal cavity was closed in two layers with 5-0 sutures. Postoperatively, mice received 1 ml of pre-warmed sterile saline via subcutaneous injection for fluid resuscitation and were maintained at 37˚C for thermal support.

Control mice underwent identical surgical procedures, including cecal exteriorization, but without ligation or puncture. The monitored parameters included body temperature, mobility, food/water intake and pain-related behaviors, with assessments conducted hourly. Terminal blood samples (1 ml) were collected from the inferior vena cava, and liver tissues were harvested. All procedures were performed under deep anesthesia immediately prior to euthanasia. The serum obtained by centrifugation (3,000 x g for 10 min at 4˚C) and liver tissues were stored at -80˚C for future experimental use.

Euthanasia procedure. Mice were euthanized by 5% isoflurane overdose until respiratory arrest (~5 min), with mortality confirmed via cardiac cessation, absent corneal reflex and fixed pupil dilation (per AVMA Guidelines 2020) (20).

Cell culture and LPS-induced model. Both Raw264.7 cells (cat. no. YC-C020) and the RP105 (alias, CD180) knockout

cell line (cat. no. YKO-M041) were commercially obtained from Ubigene). In the present study, CRISPR/Cas9 technology was used for gene KO, with the negative control (NC) group consisting of untransfected WT cells. The RP015 KO cell line was generated by precisely deleting a 382-base pair fragment (completely removing exon 3) in clone C7 (the KO cell line was produced by Ubigene). All cells were cultured in a humidified incubator (Thermo Fisher Scientific, Inc.) maintained at 37˚C and 5% CO_2 in high-glucose Dulbecco's Modified Eagle Medium (cat. no. G4511; Wuhan Servicebio Technology Co., Ltd.) supplemented with 10% heat-inactivated fetal bovine serum (cat. no. A5256701; Gibco; Thermo Fisher Scientific, Inc.) For the experiment, the cultures were placed in the aforementioned medium overnight (at 37˚C with 5% CO_2) and 1 μg/ml LPS (InvivoGen) was administered when the cells reached 80-90% confluence, with treatment for 24 h.

H&E. After washing the excised liver tissues, which were stored at -80˚C, with sterile normal saline, they were fixed in 4% buffered paraformaldehyde at room temperature for 24 h, then embedded in paraffin for subsequent processing. All paraffin-embedded sections were cut to 4-μm thickness, stained with H&E at room temperature. After dewaxing and rehydration (Sections were sequentially dehydrated through a graded ethanol series (100, 95, 80, 70%) and finally immersed in distilled water for 5 min to achieve rehydration), stain the sections were incubated with hematoxylin for 5 min, then eosin for 15 min, both at room temperature, followed by observation and imaging using a light microscope. Two pathologists, blinded to the experimental groups, randomly selected three different fields of view to evaluate the liver injury of each animal. The liver injury score was used to assess the characteristics of sepsis-induced liver injury, and the pathological scoring was carried out according to previous studies (21,22). The degrees of inflammatory infiltration, thrombosis and necrosis were graded separately (0 was defined as absent and four as severe). The total score of liver histological scoring was expressed as the sum of the scores of each parameter, with a maximum of 12 points.

Biochemical analysis. Serum samples stored at -80˚C were thawed at room temperature for 30 min. After complete thawing, they were centrifuged at low speed (750 x g for 30 sec at 4˚C), gently mixed by vortexing and air bubbles in the tubes were thoroughly aspirated to prevent interference with the experimental results. Subsequently, standardized processing and streamlined detection were conducted by professional medical technicians using a fully automated biochemical analyzer. Serum levels of alanine aminotransferase (ALT) and aspartate aminotransferase (AST) were measured using the BS-2000 automatic biochemical analyzer (Shenzhen Mindray Bio-Medical Electronics Co., Ltd.). All detection procedures were carried out at the Experimental Center of Zhongnan Hospital, Wuhan University (Wuhan, China).

Reverse transcription quantitative PCR (RT-qPCR). Total RNA was extracted from liver tissues of the mice using the Trizol kit (cat. no. R0016; Beyotime Institute of Biotechnology), followed by reverse transcription of the RNA into cDNA using the Hifair® V one-step RT-gDNA digestion SuperMix kit (cat. no. 11142ES10; Shanghai Yeasen Biotechnology Co., Ltd.). A total of 1 μg RNA was used for cDNA conversion. The reverse transcription procedure was carried out as follows: Initial primer annealing at 30˚C for 5 min, followed by cDNA synthesis at 55˚C for 30 min and final enzyme inactivation at 85˚C for 5 min. qPCR was carried out using SYBR Green dye (Biosharp Life Sciences). The qPCR amplification protocol consisted of an initial denaturation step at 95˚C for 5 min, followed by 40 cycles of denaturation at 95˚C for 10 sec and annealing/extension at 60˚C for 30 sec with fluorescence signal acquisition. Relative gene expression levels were determined using the $2^{-\Delta\Delta Cq}$ (23) method and normalized to the β-actin reference gene. The primers for the target genes are listed in Table I.

Immunohistochemistry (IHC). Liver tissue was first fixed in 4% paraformaldehyde for 24 h (at room temperature), embedded in paraffin and sliced into sections of 4-μm thickness. These sections were dewaxed, rehydrated for 30 min at room temperature, blocked with 3% BSA for 30 min at 37˚C, and finally incubated overnight at 4˚C with primary antibodies: anti-RP105 (1:1,000; cat. no. ab184956; Abcam) and anti-Caspase3 (1:200; cat. no. 19677-1-AP; Proteintech Group, Inc.). The slides were then incubated with Goat Anti-Rabbit IgG H&L (1:1,000; cat. no. ab205718; Abcam) at 37˚C for 1 h. Immunoreactivity was visualized using 3,3-diaminobenzidine tetrahydrochloride, which produces a brown precipitate at the antigen site. Subsequently, the cell nuclei were re-counterstained with Mayer's Hematoxylin Stain Solution (cat. no. G1080; Beijing Solarbio Science & Technology Co., Ltd.) at room temperature for 1 min, the slides were dehydrated and cells were observed and imaged under a light microscope.

Immunofluorescence (IF). IF followed a protocol similar to that reported previously (24). The sections were prepared following the same protocol as used for IHC; they were then incubated (overnight at 4˚C) with anti-myeloperoxidase (MPO; 1:100; cat. no. 22225-1-AP; Wuhan Sanying Biotechnology), anti-F4/80 (1:5,000; cat. no. ab300421; Abcam) and anti-suppressor of cytokine signaling 2 (SOCS2; 1:1,000; cat. no. A9190; ABclonal Biotech Co., Ltd.). After washing to remove the unbound antibody, the slides were incubated with a secondary antibody (1:1,000; cat. no. ab205718; Abcam) conjugated to Alexa Fluor 594 (cat. no. ab150080; Abcam) or XFD488 tyramide reagent (100 μl was applied to each sample and they were incubated for 5-10 min at room temperature; cat. no. 11070; AAT Bioquest, Inc.). Next, nuclei were stained with DAPI. Finally, the slides were observed and imaged under a fluorescence microscope.

Western blotting (WB). Precooled RIPA lysis buffer (Wuhan Servicebio Technology Co., Ltd.) was added to a sterile centrifuge tube, along with grinding beads. Frozen liver tissue (30-50 mg) was added to a centrifuge tube, followed by grinding to obtain a homogenate (the entire operation was carried out on ice). After grinding, the centrifuge tube was transferred to a refrigerated centrifuge and centrifuged at 12,000 x g for 15 min at 4˚C. After centrifugation, the supernatant was

Table I. Primer sequences of the target genes.

Gene	Forward primer sequence (5'-3')	Reverse primer sequence (5'-3')
IL-1β	CACCTCACAAGCAGAGCACAAG	GAAACAGTCCAGCCCATACTTTAGG
IL-6	CTTCTTGGGACTGATGCTGGTGAC	TCTGTTGGGAGTGGTATCCTCTGTG
TNF-α	AAGACACCATGAGCACAGAAAGC	GCCACAAGCAGGAATGAGAAGAG
RP105	GACCAACTCACTTCAGACA	TGACTAAGAGCCTCAATGC
β-Actin	CAGCAAGCAGGAGTACGATGAGTC	CAGTAACAGTCCGCCTAGAAGCAC

carefully aspirated, which served as the protein extract. The total protein concentration was determined using the BCA method. For electrophoresis, 30 μg of protein per lane was loaded for animal tissue samples, and 50 μg of protein per lane was loaded for cell samples. After separating proteins with different molecular weights using SDS-PAGE (10 and 12%), the proteins were electrically transferred onto a PVDF membrane. Following a 2-h blocking treatment of the membrane with 5% BSA solution, the membrane was incubated overnight with a specific primary antibody at 4˚C. Subsequently, followed by labeling with Goat Anti-Rabbit IgG H&L (1:5,000, cat. no. AS014; ABclonal Biotech Co., Ltd.). Finally, the protein bands on the membrane were visualized using ECL (Biosharp Life Sciences). Briefly, the membranes were incubated overnight at 4˚C with the following corresponding primary antibodies: Anti-RP105 (1:1,000, cat. no. ab184956; Abcam), anti-SOCS2 (1:1,000; cat. no. A9190; ABclonal Biotech Co., Ltd.), anti-JAK2 (1:1,000, cat. no A11497; ABclonal Biotech Co., Ltd.), BCL-2 (1:1,000; cat. no. 26593-1-AP; Wuhan Sanying Biotechnology), anti-BAX (1:1,000; cat. no. T40051; Abmart Pharmaceutical Technology Co., Ltd.), anti-p53 upregulated modulator of apoptosis (PUMA; 1:1,000, cat. no. A3752; ABclonal Biotech Co., Ltd.), anti-Growth Arrest and DNA Damage-inducible α (GADD45A; 1:500, cat. no. A13487; ABclonal Biotech Co., Ltd.), anti-phosphorylated-JAK2 (p-JAK2; 1:2,000; cat. no. 4406; Cell Signaling Technology, Inc.), anti-STAT3 (1:1,000; cat. no. 30835; Cell Signaling Technology, Inc.), anti-phosphorylated (p-STAT3) (1:2,000, cat. no. 9145; Cell Signaling Technology, Inc.) and anti-β-actin (1:50,000, cat. no. AC026; ABclonal Biotech Co., Ltd.) antibodies.

RNA sequencing (RNA-seq). RNA was extracted from the animal tissues of the four groups, using Trizol which was the same as in RT-qPCR experiment. RNA integrity was evaluated by using the RNA Nano 6000 assay kit from Bioanalyzer After confirming RNA quality, mRNA was enriched from total RNA using poly-T oligonucleotide-attached magnetic beads (cat. no. N401-01/02; Vazyme Biotech Co., Ltd.). The purified mRNA was then fragmented and used for cDNA synthesis. First-strand cDNA was generated with random hexamer primers and M-MuLV Reverse Transcriptase (RNase H^-) (Fast RNA-seq Lib Prep Kit V2; cat. no. RK20306; ABclonal Biotech Co., Ltd.), followed by second-strand synthesis using the same kit. Adapter sequences were ligated to construct the sequencing library. High-throughput sequencing was performed on an Illumina NovaSeq platform using the NovaSeq X Plus 25B Reagent Kit (300 cycles; cat. no. 20104706; Illumina Inc.) to generate 150 bp paired-end reads. The final library was loaded at a concentration of 80-120 pM. Following construction, libraries were quantified (Qubit 2.0 Fluorometer; Thermo Fisher Scientific, Inc.), diluted to 1.5 ng/μl, assessed for insert size (Agilent 2100 Bioanalyzer; Agilent Technologies, Inc.) and finally quantified for effective concentration (>1.5 nM) by quantitative PCR. After obtaining the RNA-seq gene expression matrix, differential expression analysis was carried out using the DESeq2 R package (1.20.0; https://github.com/mikelove/DESeq2). The CLP-treated WT group (CLP group) and CLP-treated RP105 knockout group (RP105 KO + CLP group) were selected for differential gene comparison analysis, aiming to explore the molecular mechanism by which RP105 exerts its effects on mice in the CLP model. Differentially expressed genes (DEGs) were screened by two simultaneous criteria: Absolute log2 fold change (log2FC)≥1 (ensuring biologically significant expression changes) and adjusted P-value (Padj) <0.05 (controlling false positives and ensuring statistical reliability). Raw sequencing data generated in the present study are available in the GEO database (dataset no. GSE298411; https://www.ncbi.nlm.nih.gov/gds/?term=GSE298411).

Co-immunoprecipitation (Co-IP). After thorough grinding, the mouse liver tissue (30-50 mg) was lysed with 200 μl immunoprecipitation lysis buffer on ice for 30 min using immunoprecipitation lysis buffer (cat. no. BK0004-02; Boyi Bio ACE.). The lysate was then subjected to centrifugation at 4 x g for 10 min at 4˚C. The resulting supernatant, which contained the protein sample, was mixed with SOCS2 antibody (1:1,000; A9190; ABclonal Biotech Co., Ltd.) and incubated overnight at 4˚C. Next, 20 μl of Protein A/G agarose beads were added to the antibody-protein mixture and incubated for an additional 1 h at room temperature. The complexes were then separated using magnetic bead-based isolation, followed by elution and denaturation procedures according to the manufacturer's instructions (cat. no. BK0004-02; Boyi Bio ACE) and analyzed by WB.

Flow cytometry. Fresh Raw246.7 cells were washed with 1 ml pre-cooled PBS at 4˚C by pipetting, followed by centrifugation at 1,000-1,500 x g for 5 min at 4˚C to collect the cells. The washing step was repeated twice. A volume of 100 μl 1X binding buffer (cat. no. G1511-50T; Wuhan Servicebio Technology Co., Ltd.) working solution was added to the cell pellet to resuspend the cells. Cells were then mixed thoroughly with 5 μl of Annexin V-FITC and 5 μl of Propidium Iodide. The mixture was incubated in the dark at room temperature

for 15 min. After staining and incubation, 400 μl 1X Binding Buffer working solution was added to each tube, mixed well and samples were analyzed using a flow cytometer (CytoFLEX; Beckman Coulter, Inc.). Data were analyzed using FlowJo software (V10.8; BD Biosciences).

Statistical analysis. Statistical analysis was carried out using GraphPad Prism 8.0 software (Dotmatics). All data are presented as the mean ± standard deviation. Differences between groups were analyzed using two-way ANOVA. $P<0.05$ was considered to indicate a statistically significant.

Results

Knockout of RP105 exacerbates hepatic inflammation and injury in the CLP model. To clarify the specific effect of RP105 on the liver during sepsis, a septic mouse model was induced using CLP and was used to evaluate the functional status of hepatocytes in the liver. A schematic diagram of the animal experiment is shown in Fig. 1A. The knockout efficiency was verified in the liver of RP105 KO mice using IHC and qPCR (Fig. 1B-D). Examination of serum ALT and AST levels, indicators of liver function damage, revealed that ALT and AST levels were significantly increased in RP105 KO + CLP mice (ALT, 109.0±15.66; AST, 387.7±37.92) compared with the CLP group (ALT, 62.7±4.20; AST, 218.1±27.96; Fig. 1E and F). Moreover, the observations revealed significant pathological changes in the liver of RP105 KO + CLP mice, including severe edema, sinusoidal congestion and pronounced hepatocellular necrosis. By contrast, mice in the CLP group exhibited only mild to moderate edema and sinusoidal congestion (Fig. 1G and H). These findings suggest that RP105 carries out a key role in maintaining normal liver structure and function during sepsis.

To further demonstrate the role of RP105 in septic liver injury, additional analysis of inflammatory cell infiltration was conducted by measuring classic markers of inflammation, MPO and F4/80. Compared with the CLP group (MPO, 0.2562±0.0663; F4/80, 0.2408±0.0487), a significant increase in the expression levels of these markers was observed in the liver tissues of RP105 KO mice (MPO, 0.4306±0.0847; F4/80, 0.3776±0.0552), confirming the intensified infiltration of inflammatory cells in the liver (Fig. 2A-D). Furthermore, qPCR technology was used to assess the expression levels of key pro-inflammatory cytokines such as IL-1β, IL-6 and TNF-α. The results indicated that, compared with the CLP group (IL-1β, 9.59±0.92; IL-6, 11.51±3.54; TNF-α, 5.70±0.66), RP105 KO + CLP mice (IL-1β, 15.61±2.66; IL-6, 66.84±9.99; TNF-α, 12.12±3.42) exhibited significantly elevated levels of pro-inflammatory cytokines (Fig. 2E-G). These finding highlights the key role of RP105 in regulating the balance between inflammatory responses.

Knockout of RP105 aggravates hepatocyte apoptosis in the CLP model. Accordingly, the level of apoptosis in the mouse liver was measured. Analysis of the IHC experiment revealed that, compared with the CLP group, there was enhanced expression of Caspase3 in the RP105 KO + CLP group (Fig. 3A and B). Furthermore, compared to the CLP group, the ratios of the apoptosis-related proteins GADD45A, PUMA and BAX to BCL2 were significantly upregulated in the RP105 KO + CLP group (Fig. 3C-F), further confirming the activation of the apoptotic signaling pathway. These findings emphasize that, in the context of sepsis, the absence of RP105 exacerbates apoptosis in the mouse liver, highlighting the protective role of RP105 against hepatic damage in an inflammatory condition.

RP105 exhibits the ability to interact with SOCS2. Following RP105 knockout, the liver function impairment, inflammatory response and apoptosis observed in the mouse CLP model were exacerbated. To explore the potential mechanisms of RP105 in this model, three samples from each of the two groups (CLP and RP105 KO + CLP groups) were randomly selected and RNA-seq analysis was carried out. To visually represent these DEGs, heatmaps were created for clustering analysis (Fig. 4A). The volcano plot revealed 320 DEGs between the CLP and RP105 KO + CLP groups, with 180 upregulated and 140 downregulated genes (Fig. 4B). Notably, significant upregulation of SOCS2 gene expression was observed within the upregulated gene set in CLP model mice compared with the RP105 KO + CLP group (Fig. 4A and B), which warrants further investigation. Current evidence indicates that SOCS2 carried out a key anti-inflammatory regulatory role. For instance, SOCS2 suppresses inflammation and apoptosis during nonalcoholic steatohepatitis progression by restricting NF-κB activation in macrophages (25). More importantly, studies have identified SOCS2 as a feedback inhibitor of TLR-induced activation, capable of specifically suppressing TLR signaling pathway activation (26,27), a mechanism associated with the immune function of RP105 (15,28,29). Although RNA-seq analysis identified multiple DEGs, pathway enrichment analysis and literature review revealed that other upregulated DEGs revealed weaker direct associations with inflammatory regulation. Therefore, SOCS2 was ultimately selected as the core target for subsequent mechanistic investigations.

To further explore the interplay between RP105 and SOCS2, Co-IP was carried out. This experiment revealed that SOCS2 specifically binds to RP105 in mouse tissue samples, providing preliminary evidence for a direct interaction between the two proteins (Fig. 4C). To strengthen this conclusion, a comparative Co-IP experiment was carried out using liver samples from RP105 KO and WT mice. This approach enabled the direct assessment of the effect of RP105 deficiency on the binding capacity of SOCS2. The experimental results revealed that the specific binding between SOCS2 and RP105, observed in the WT mouse liver, completely disappeared following RP105 knockout (Fig. 4D). This finding not only corroborates the initial results but also suggests the existence of an interaction between RP105 and SOCS2.

Reduction of SOCS2 expression in sepsis liver by knockdown of RP105. To validate the RNA-seq analysis, SOCS2 protein expression levels across four groups: WT, RP105 KO, CLP and RP105 KO + CLP groups as assessed. IHC and WB was employed to provide direct evidence of the differential expression of SOCS2 under various treatment conditions (Fig. 5A-E), not only to gain a deeper understanding of the subcellular localization of the SOCS2 protein, but also to observe potential alterations in its intracellular distribution

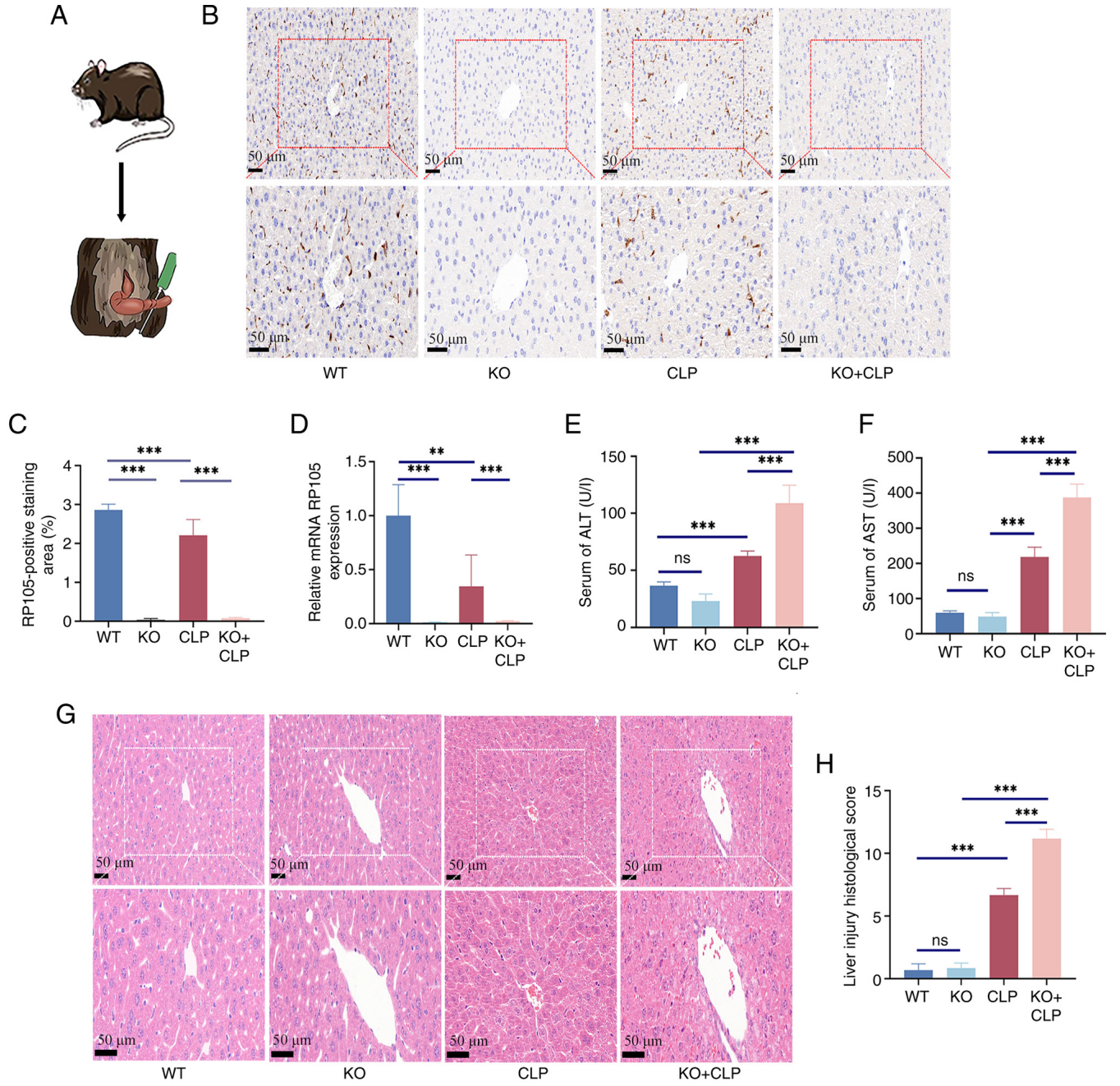

Figure 1. Knockout of RP105 exacerbates hepatic injury in the CLP model. (A) Simplified diagram of CLP in mice. (B) IHC staining of RP105 was carried out on a paraffin-embedded section of the liver tissues of mice. (C) IHC staining of RP105 was quantified using Image-Pro Plus 6.0. (D) mRNA expression levels in the liver of RP105 was tested by reverse transcription-quantitative PCR. The levels of (E) ALT and (F) AST in serum. (G) H&E staining and histological injury score in mouse liver tissue. (H) Histological scores. Ns, P>0.05, **P<0.01 and ***P<0.001. CLP, cecal ligation and puncture; IHC, immunohistochemical; WT, wild-type; KO, knockout; AST, aspartate aminotransferase; ALT, alanine aminotransferase; RP105, radioprotective 105.

pattern under conditions of sepsis and RP105 knockout. After CLP surgery, SOCS2 expression was significantly increased in the liver of mice. Although RP105 expression was reduced in the CLP group when compared with the WT group, SOCS2 expression was still markedly elevated, likely due to the activation of SOCS2 expression by CLP-induced inflammation. However, in the RP105 KO + CLP group, SOCS2 expression was significantly suppressed. Despite this, SOCS2 expression in the RP105 KO + CLP group was still increased compared with that in the knockout group (Fig. 5A-E), suggesting that in the inflammatory environment, SOCS2 expression is not only regulated by RP105 but may also be influenced by other complex signaling pathways.

RP105 mediates SOCS2 expression to hepatic inflammation and injury in the CLP model through the JAK2/STAT3 pathway. In a murine model of sepsis, RNA-seq analysis revealed significant differential expression of SOCS2 between RP105 knockout mice and wild-type controls (Fig. 4A and B). SOCS2 serves as a negative feedback regulator within the complex regulatory network of cytokine signaling. The classic negative feedback regulatory signaling pathway involves

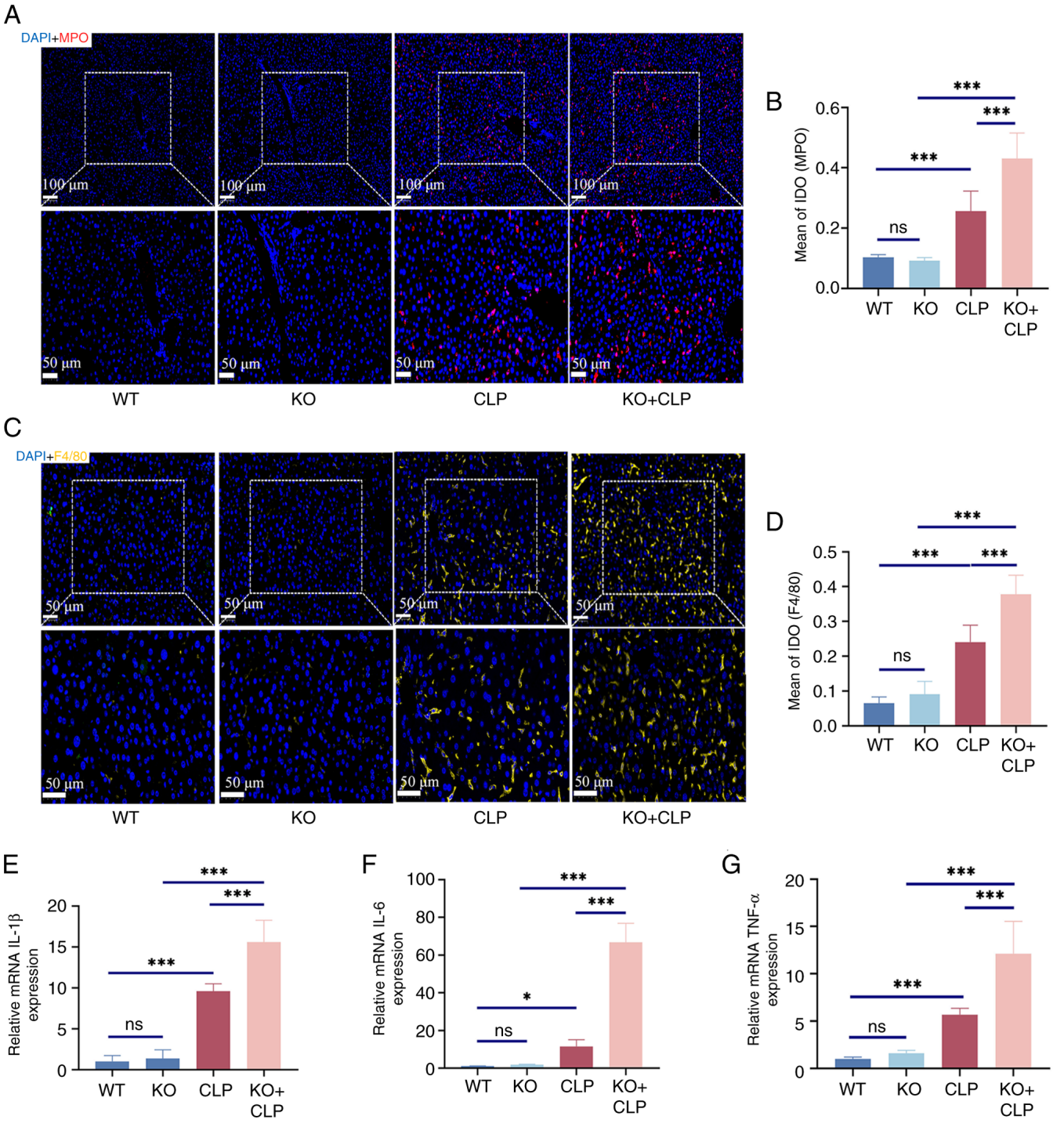

Figure 2. KO of RP105 exacerbates hepatic inflammation in the CLP model. (A) IF staining of MPO was carried out on a paraffin-embedded section of the liver tissues of mice. (B) IF stained fluorescence of MPO was quantified using Image-pro plus 6.0. (C) IF staining of F4/80 was carried out on a paraffin-embedded section of mouse liver tissues. (D) IF stained fluorescence of F4/80 was quantified using Image-pro plus 6.0. mRNA expression levels in the liver of (E) IL-1β, (F) IL-6 and (G) TNF-α were tested by reverse transcription-quantitative PCR. Ns, P>0.05, *P<0.05 and ***P<0.001. CLP, cecal ligation and puncture; WT, wild-type; KO, knockout; MPO, anti-myeloperoxidase; IF, immunofluorescence; RP105, radioprotective 105.

the activation of the JAK2/STAT3 pathway. Building upon this finding, in-depth functional validation of the canonical SOCS2-mediated JAK2/STAT3 signaling pathway was conducted.

To confirm the function of RP105 and its role in sepsis-induced liver injury through inactivation of the JAK2/STAT3 pathway via the upregulation of SOCS2, WB experiments were conducted on liver tissues from the four groups to accurately assess the expression levels of JAK2, p-JAK2, STAT3 and p-STAT3. WB indicated that, in the absence of CLP treatment, there were no significant differences in the basal expression levels of JAK2 and STAT3 among the groups. However, a remarkable change was observed following CLP surgery: In the RP105 KO + CLP group, the phosphorylation levels of JAK2 and STAT3 were significantly elevated compared with the CLP group (Fig. 6A-C).

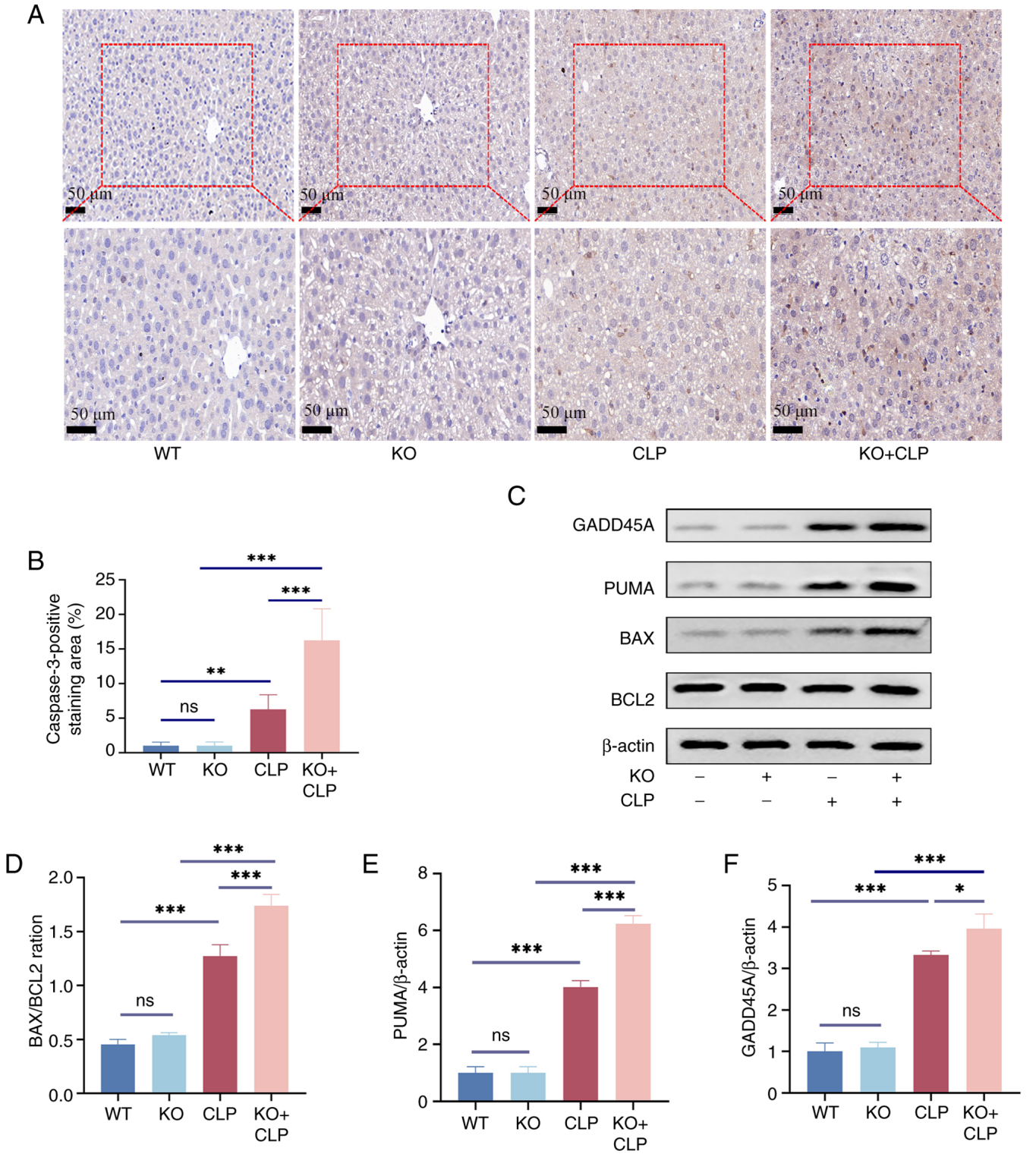

Figure 3. KO of RP105 aggravates hepatocyte apoptosis in the CLP model. (A) IHC staining of Caspase3 was carried out on a paraffin-embedded section of the mice liver tissues. (B) IHC-stained fluorescence of Caspase3 was quantified. (C) Representative images of western blotting and analysis of (D) BAX/BCL2 ratio. (E) PUMA and (F) GADD45A as a ratio of β-actin proteins. Expression. ns, P>0.05, *P<0.05, **P<0.01 and ***P<0.001. CLP, cecal ligation and puncture; WT, wild-type; KO, knockout; IHC, immunohistochemical; RP105, radioprotective 105.

RP105 regulates the inflammatory response of LPS-induced RAW264.7 macrophages by modulating the SOCS2/JAK2/STAT3 pathway. To verify *in vitro* whether RP105 can ameliorate the inflammatory response in sepsis by regulating the SOCS2/JAK2/STAT3 pathway, the expression of relevant proteins in RAW264.7 cells after LPS stimulation were assessed. Flow cytometry analysis of the cellular model revealed that, compared with normal cells, RAW264.7 macrophages with RP105 knocked out exhibited a significant increase in apoptosis rate after LPS stimulation (Fig. 7A and B). WB revealed that the changes in protein expression within this pathway were similar to those observed at the animal level (Fig. 7C-G).

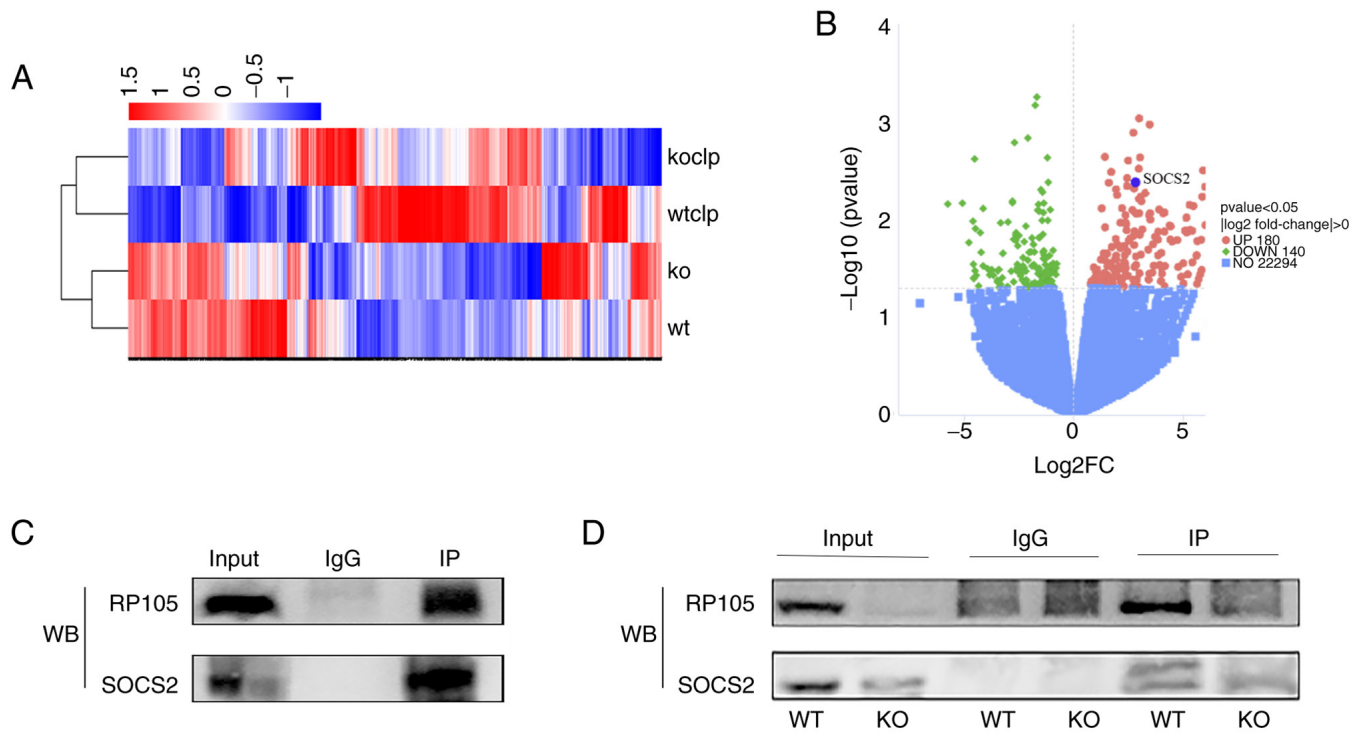

Figure 4. RP105 exhibits the ability to interact with SOCS2. (A) Heatmap of cluster analysis. (B) Volcano plot of differential gene expression. Among them, SOCS2 is significantly upregulated. (C) Co-IP analysis of the interaction between RP105 and SOCS2 in WT mouse tissues. (D) Co-IP analysis of the interaction between RP105 and SOCS2 in WT and RP105 KO mice tissues. RP105, radioprotective 105; SOCS2, suppressor of cytokine signaling 2; WT, wild-type; KO, knockout; WB, western blotting.

Discussion

Sepsis is a systemic inflammatory response syndrome triggered by pathogenic microorganisms, such as bacteria (30). When these pathogens invade the body, they release toxins that activate the immune system of the host. Excessive release of inflammatory mediators and cytokines leads to a systemic inflammatory response, which can result in multiple organ dysfunction (31). Impaired liver function is closely associated with the prognosis of sepsis and serves as a robust independent predictor of mortality (32). Understanding the changes in liver function during sepsis is key to improving the survival rates of patients with sepsis. The present study selected CLP as an animal model for sepsis to simulate the septic environment *in vivo*, as it is widely regarded as the gold standard for sepsis research (33-35).

RP105 was initially identified as a surface marker of B cells in mice and humans (36). It belongs to a class of type I transmembrane receptors and exhibits substantial structural similarity to TLRs. Similar to TLR4, RP105 contains abundant LRRs (10), which are common structural domains found in several proteins. The LRR domain carries out a key role in protein-protein interactions through its specific three-dimensional structure (37), facilitating the recognition and activation of various immune responses and interactions with exogenous pathogens (38). By sensing extracellular stimuli, RP105 acts as a bridge to transmit signals to the intracellular effectors. As a TLR homolog, RP105 carries out a key role in the negative regulation of inflammation. Although the beneficial effects of RP105 have been well established in TLR4-dependent contexts, recent data have also highlighted its roles in TLR4-independent pathways (19,39,40). RP105 possesses pathways independent of TLR4 signal transduction and can physically interact with the PI3K pathway, carrying out a significant role in improving myocardial ischemia-reperfusion injury through the PI3K/AKT pathway (41).

Building on the established role of RP105 in the anti-inflammatory process (14), the potential of RP105 as a therapeutic target for modulating septic liver injury was investigated. The study revealed that RP105 is key for protecting liver function. Compared with the control group, RP105 knockout mice exhibited aggravated liver dysfunction after CLP treatment, accompanied by relevant histopathological changes and a more intense inflammatory response. This is consistent with previous studies that have emphasized the role of RP105 as a negative regulator of inflammation (13,42-44). Further RNA-Seq results revealed that among the DEGs, SOCS2 was downregulated in RP105 KO mice. Co-IP experiments demonstrated that SOCS2 specifically binds to RP105 in mouse tissues. This was confirmed by comparative Co-IP using liver samples from RP105 KO and WT mice: The SOCS2-RP105 binding observed in WT liver disappeared after RP105 knockout, suggesting an interaction.

To validate the results of RNA-seq analysis, an in-depth assessment of SOCS2 protein expression levels across four experimental groups was conducted: WT, RP105 KO, CLP and RP105 KO + CLP. Analysis revealed an apparent paradox in SOCS2 expression: While CLP surgery alone induced a significant upregulation of SOCS2 in the liver, its expression was markedly reduced in RP105 KO + CLP mice. This finding suggests that the induction of SOCS2 during sepsis may require the presence of RP105. One possible explanation

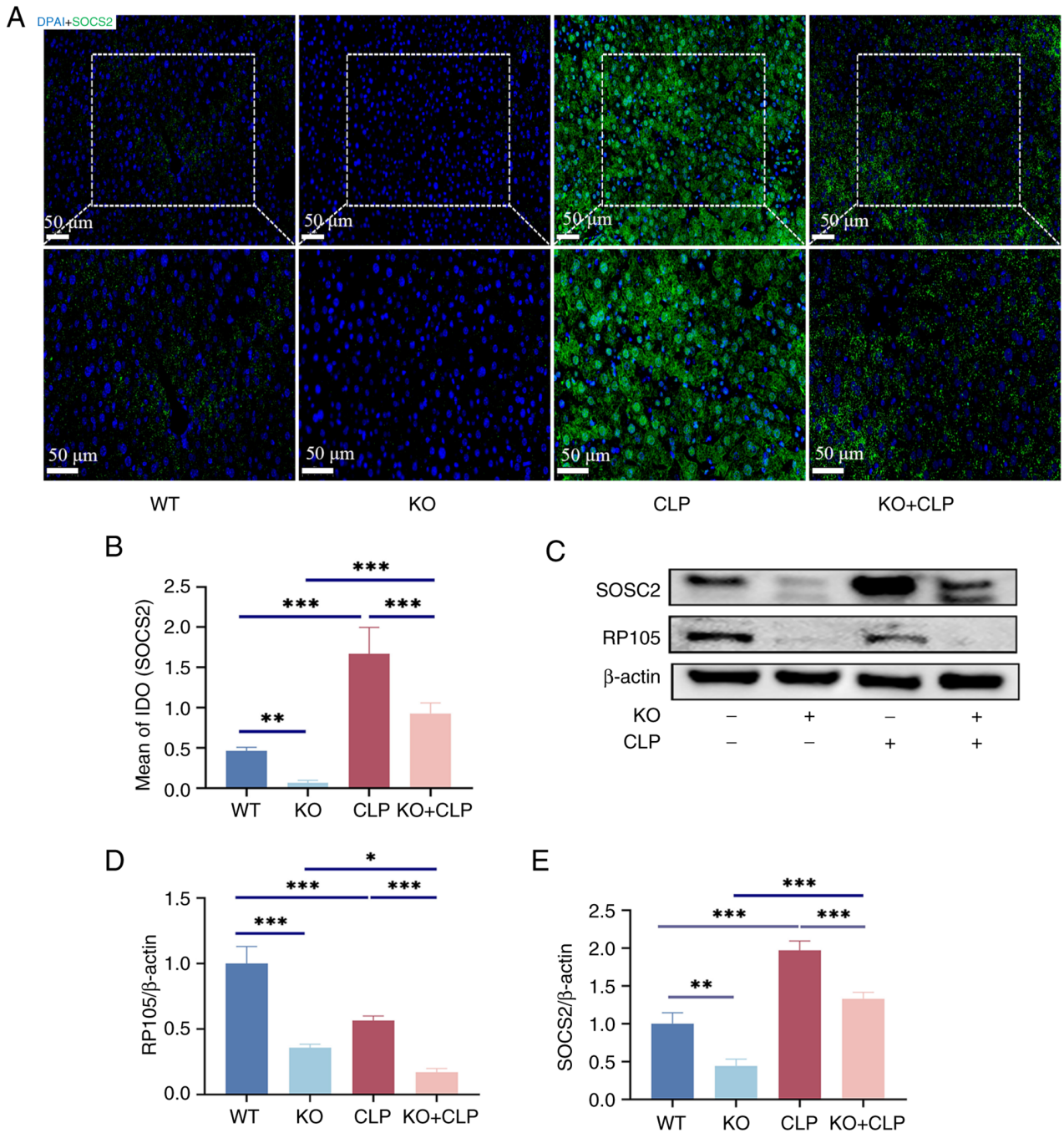

Figure 5. RP105 exhibits the ability to interact with SOCS2 and reduce SOCS2 expression in the liver of sepsis by knockdown of RP105. (A) IF staining of SOCS2 was carried out on a paraffin-embedded section of the mice liver tissues. (B) IF-stained fluorescence of SOCS2 was quantified using Image-pro plus 6.0. (C) Representative images of western blotting and analysis of (D) RP105, (E) SOCS2 protein expression as a ratio of β-actin protein expression. *P<0.05, **P<0.01 and ***P<0.001. RP105, radioprotective 105; SOCS2, suppressor of cytokine signaling 2; WT, wild-type; KO, knockout; CLP, cecal ligation and puncture.

is that under inflammatory stress, RP105 facilitates SOCS2 expression, possibly through a direct interaction, as supported by the Co-IP results demonstrating specific binding between RP105 and SOCS2. In the absence of RP105, this regulatory axis may be disrupted, leading to an insufficient upregulation of SOCS2 in response to the strong inflammatory stimulus induced by CLP. Consequently, as shown by the increased phosphorylation of JAK2 and STAT3 in RP105 KO + CLP mice, the JAK2/STAT3 signaling pathway becomes hyperactivated, further aggravating liver inflammation and injury. Together, these data suggest that RP105 is important not only for maintaining hepatic homeostasis during sepsis but also for ensuring appropriate SOCS2 induction to restrain cytokine-mediated damage. Notably, despite the suppression of SOCS2 expression in the CLP group with RP105 knockout, SOCS2 expression was still increased in the RP105 KO + CLP group. This finding suggests that in an inflammatory environment, SOCS2 expression is not only regulated by RP105 but also is influenced by other complex pathways. For instance, inflammatory cytokines such as IL-1β may induce SOCS2 expression through alternative signaling pathways (45).

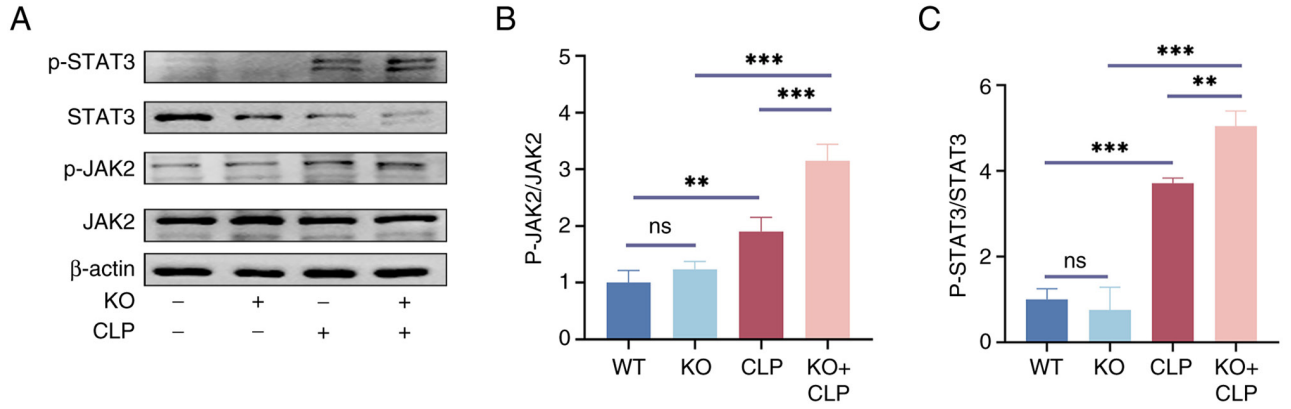

Figure 6. RP105 mediates SOCS2 expression in hepatic inflammation and injury in the CLP model through the JAK2/STAT3 pathway. (A) Representative images of western blotting and analysis of (B) p-JAK2/JAK2 and (C) p-STAT3/STAT3. ns, P>0.05, *P<0.05, **P<0.01 and ***P<0.001. p, phosphorylated; WT, wild-type; KO, knockout; CLP, cecal ligation and puncture.

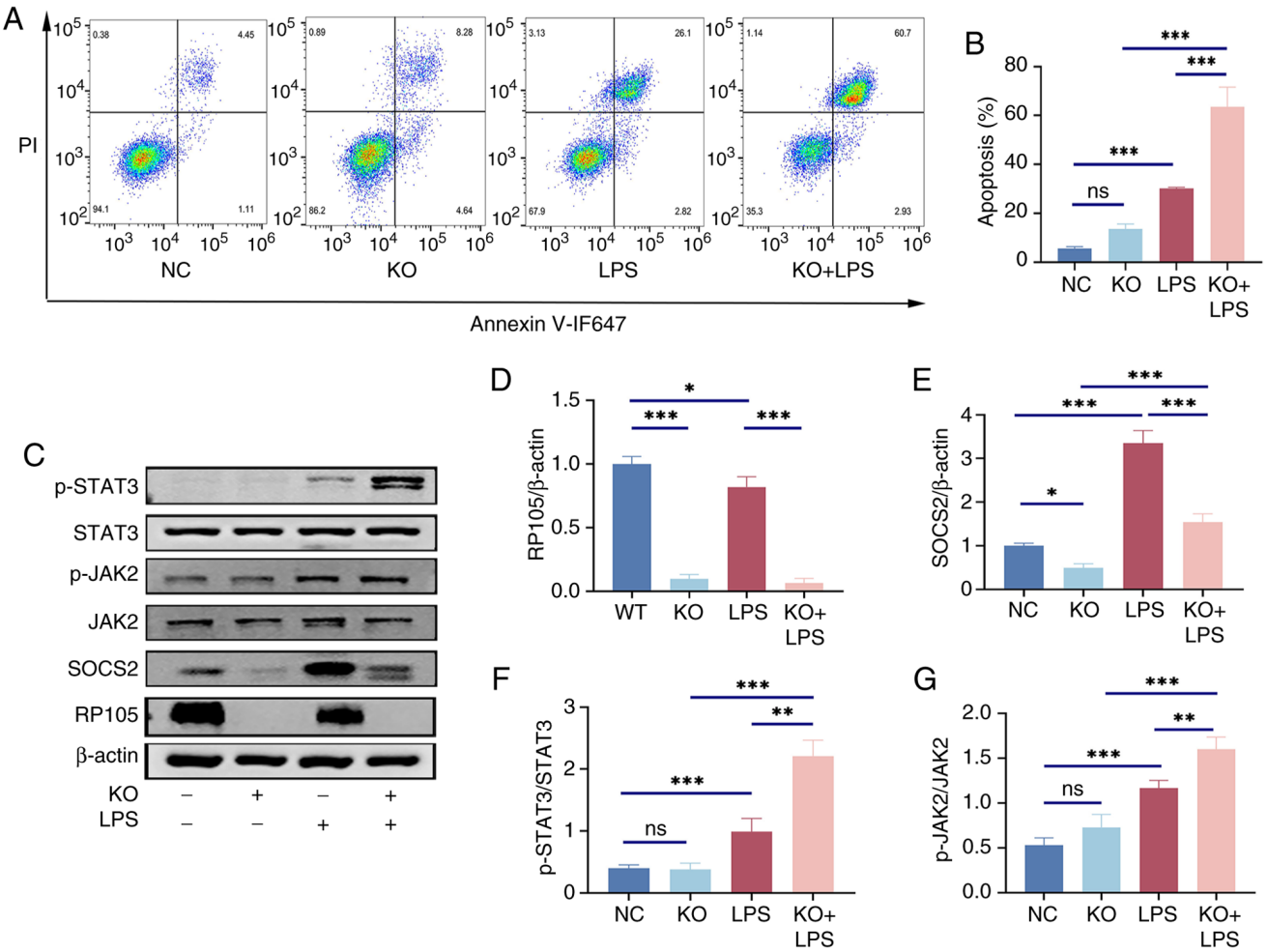

Figure 7. RAW264.7 cells with KO of RP105 gene expression exhibits exacerbated damage from LPS under the influence of the JAK2/STAT3 signaling pathway. (A) Representative flow cytometric images and (B) analysis of apoptosis after LPS treatment in RAW264.7 cells. (C) Representative western blotting images and analysis of (D) RP105/β-actin, (E) SOCS2/β-actin, (F) p-JAK2/JAK2 and (G) p-STAT3/STAT3. ns, P>0.05, *P<0.05, **P<0.01 and ***P<0.001. LPS, lipopolysaccharide; NC, negative control; KO, knockout; RP105, radioprotective 105; SOCS2, suppressor of cytokine signaling 2.

Additionally, in the CLP group, despite a decrease in RP105 expression compared with the WT group, SOCS2 expression significantly increased. This may be due to the inflammatory environment triggered by CLP surgery activating SOCS2 expression, which may override the regulatory effect of RP105 on SOCS2. However, this also raises the possibility that RP105 is not the sole upstream regulator of SOCS2 and inflammatory cues such as IL-1β or IL-6 may independently enhance SOCS2 expression through STAT-dependent transcription. Such a compensatory induction, though present, appears insufficient

to suppress downstream signaling in the absence of RP105. In summary, the present study not only validates the results of RNA-seq analysis but also uncovers the complex regulatory mechanisms of SOCS2 in inflammatory responses and the pivotal role of RP105 in this process. These observations suggest that the RP105-SOCS2 interaction may serve as a regulatory checkpoint that constrains excessive activation of the JAK2/STAT3 axis during septic liver injury. The disruption of this checkpoint in RP105-deficient conditions may contribute to signal amplification, cytokine storm and hepatocyte apoptosis. These findings provide new insights into the understanding of the inflammatory responses and the search for potential therapeutic targets.

SOCS2, operates within classic feedback loops by targeting the degradation of signaling intermediates, thereby blocking further signal transduction (46). Imbalances in these proteins can lead to a wide range of pathological changes, highlighting the essential role of SOCS2 in regulating cell fate and inflammatory processes (47). As a pivotal signaling protein, SOCS2 exhibits diverse functions across various cell types (48,49), underscoring its importance. Notably, SOCS2 carries out a key role in modulating immune responses and inflammatory pathways, which are vital for maintaining organismal health (50). Previous research (25) has reported that SOCS2 in macrophages exerts anti-inflammatory and anti-apoptotic effects by modulating the NF-κB signaling pathway, while also attenuating inflammation through the inhibition of the inflammasome signaling pathway. Additionally, SOCS2 has been revealed to be vital in balancing immune responses and protecting against oxidative stress during acetaminophen-induced acute liver injury, acting as a key regulatory factor in liver immune responses following acetaminophen therapy (51).

SOCS2 serves as a negative feedback regulator within the complex regulatory network of cytokine signaling. By interacting precisely with core molecules in the signaling complex, it effectively blocks further extension of the signaling chain, achieving negative feedback regulation of the cytokine signaling pathway. A classic example of this regulatory mechanism is the activation of the JAK/STAT pathway. During inflammation, SOCS2 forms complexes with key proteins in the JAK/STAT pathway, thereby effectively inhibiting the amplification and transmission of inflammatory signals. This ensures timely termination and precise regulation of cellular responses to inflammatory factors, thus inhibiting inflammatory reactions. We hypothesize that the JAK2/STAT3 pathway carries out a key role in protecting against liver injury due to sepsis mediated by RP105 through SOCS2. In the present study, we found that the phosphorylation levels of JAK2/STAT3 in the liver tissues of RP105 KO mice subjected to the CLP model and in RAW264.7 macrophages treated with LPS were both increased compared with those in the control groups. This consistent activation across *in vivo* and *in vitro* systems suggests that SOCS2 carries out a non-redundant role in restraining this pathway, and its suppression in the absence of RP105 may permit uncontrolled signaling propagation. These findings suggest that RP105 mitigates the progression of sepsis-induced liver injury through the inactivation of the JAK2/STAT3 pathway mediated by SOCS2.

Based on the aforementioned research findings, we hypothesize that intervention methods targeting the enhancement of the RP105-SOCS2 interaction can be designed to evaluate their intervention effects in the early stage of septic liver injury. Additionally, through prospective cohort studies, the levels of RP105 and SOCS2 in patients with sepsis at the time of admission can be detected, the associations between these levels and liver injury grading as well as treatment efficacy can be analyzed, and a combined prediction model based on their expression levels can be established, which will provide reference indicators for early clinical intervention.

While the present study provides insights into the role of RP105 in sepsis pathogenesis using murine models, it is essential to recognize the inherent limitations in translating these findings to human diseases due to fundamental differences in immune regulation and pathophysiology between species. Although murine models are indispensable for mechanistic investigations, they cannot fully replicate the complexity of human sepsis, as evidenced by significant interspecies variations in TLR signaling pathways, cytokine networks and cellular immune responses.

RP105 protects against septic liver injury by binding SOCS2 to inhibit JAK2/STAT3 signaling, thereby attenuating inflammation and apoptosis. The study is the first to demonstrate the RP105-SOCS2 interaction in septic liver injury, revealing the RP105/SOCS2 axis as a potential therapeutic target.

Acknowledgements

Not applicable.

Funding

The present study was supported by the National Natural Science Foundation of China (grant nos. 82460131 and 82060122) and Natural Science Foundation of JiangXi province (grant no. 20224ACB206027).

Availability of data and materials

The data generated in the present study may be found in the GEO database under accession number GSE298411 or at the following URL: https://www.ncbi.nlm.nih.gov/gds/?term=GSE298411.

Authors' contributions

QD designed cell and animal experiments, curated data, developed methodology, conducted formal analysis and wrote the original draft. HD and QY curated data, conducted formal and software analysis and developed methodology. RC, ZF and JX collected the information and revised, conducted analyses using software tools and finalized the manuscript. HP and QX proposed the preliminary idea and design for the present study and reviewed and revised the manuscript. QD and QX confirm the authenticity of all the raw data. All authors read and approved the final manuscript.

Ethics approval and consent to participate

The present study was approved by the Ethics Committee for Laboratory Animal Welfare of the First Affiliated Hospital

of Nanchang University (approval no. CDYFY-IACUC-202407QR198).

Patient consent for publication

Not applicable.

Competing interests

The authors declare that they have no competing interests.

References

1. Rudd KE, Johnson SC, Agesa KM, Shackelford KA, Tsoi D, Kievlan DR, Colombara DV, Ikuta KS, Kissoon N, Finfer S, *et al*: Global, regional, and national sepsis incidence and mortality, 1990-2017: Analysis for the global burden of disease study. Lancet 395: 200-211, 2020.
2. Takeuchi O and Akira S: Pattern recognition receptors and inflammation. Cell 140: 805-820, 2010.
3. Raymond SL, Holden DC, Mira JC, Stortz JA, Loftus TJ, Mohr AM, Moldawer LL, Moore FA, Larson SD and Efron PA: Microbial recognition and danger signals in sepsis and trauma. Biochim Biophys Acta Mol Basis Dis 1863: 2564-2573, 2017.
4. Fajgenbaum DC and June CH: Cytokine storm. N Engl J Med 383: 2255-2273, 2020.
5. Chousterman BG, Swirski FK and Weber GF: Cytokine storm and sepsis disease pathogenesis. Semin Immunopathol 39: 517-528, 2017.
6. Protzer U, Maini MK and Knolle PA: Living in the liver: Hepatic infections. Nat Rev Immunol 12: 201-213, 2012.
7. Heymann F and Tacke F: Immunology in the liver-from homeostasis to disease. Nat Rev Gastroenterol Hepatol 13: 88-110, 2016.
8. Yan J, Li S and Li S: The role of the liver in sepsis. Int Rev Immunol 33: 498-510, 2014.
9. Elmi AN and Kwo PY: The liver in sepsis. Clin Liver Dis 29: 453-467, 2025.
10. Miyake K, Yamashita Y, Ogata M, Sudo T and Kimoto M: RP105, a novel B cell surface molecule implicated in B cell activation, is a member of the leucine-rich repeat protein family. J Immunol 154: 3333-3340, 1995.
11. Divanovic S, Trompette A, Atabani SF, Madan R, Golenbock DT, Visintin A, Finberg RW, Tarakhovsky A, Vogel SN, Belkaid Y, *et al*: Negative regulation of Toll-like receptor 4 signaling by the Toll-like receptor homolog RP105. Nat Immunol 6: 571-578, 2005.
12. Schultz TE and Blumenthal A: The RP105/MD-1 complex: Molecular signaling mechanisms and pathophysiological implications. J Leukoc Biol 101: 183-192, 2017.
13. Yang J, Yang C, Yang J, Ding J, Li X, Yu Q, Guo X, Fan Z and Wang H: RP105 alleviates myocardial ischemia reperfusion injury via inhibiting TLR4/TRIF signaling pathways. Int J Mol Med 41: 3287-3295, 2018.
14. Fan Z, Pathak JL and Ge L: The potential role of RP105 in regulation of inflammation and osteoclastogenesis during inflammatory diseases. Front Cell Dev Biol 9: 713254, 2021.
15. Zhu J, Zhang Y, Shi L, Xia Y, Zha H, Li H and Song Z: RP105 protects against ischemic and septic acute kidney injury via suppressing TLR4/NF-κB signaling pathways. Int Immunopharmacol 109: 108904, 2022.
16. Wezel A, de Vries MR, Maassen JM, Kip P, Peters EA, Karper JC, Kuiper J, Bot I and Quax PHA: Deficiency of the TLR4 analogue RP105 aggravates vein graft disease by inducing a pro-inflammatory response. Sci Rep 6: 24248, 2016.
17. Chen F, Xu W, Tang M, Tian Y, Shu Y, He X, Zhou L, Liu Q, Zhu Q, Lu X, *et al*: hnRNPA2B1 deacetylation by SIRT6 restrains local transcription and safeguards genome stability. Cell Death Differ 32: 382-396, 2025.
18. Li T, Sun H, Li Y, Su L, Jiang J, Liu Y, Jiang N, Huang R, Zhang J and Peng Z: Downregulation of macrophage migration inhibitory factor attenuates NLRP3 inflammasome mediated pyroptosis in sepsis-induced AKI. Cell Death Discov 8: 61, 2022.
19. Duo H, Yang Y, Luo J, Cao Y, Liu Q, Zhang J, Du S, You J, Zhang G, Ye Q and Pan H: Modulatory role of radioprotective 105 in mitigating oxidative stress and ferroptosis via the HO-1/SLC7A11/GPX4 axis in sepsis-mediated renal injury. Cell Death Discov 11: 290, 2025.
20. Kollias NS, Hess WJ, Johnson CL, Murphy M and Golab G: A literature review on current practices, knowledge, and viewpoints on pentobarbital euthanasia performed by veterinarians and animal remains disposal in the United States. J Am Vet Med Assoc 261: 733-738, 2023.
21. Gong S, Yan Z, Liu Z, Niu M, Fang H, Li N, Huang C, Li L, Chen G, Luo H, *et al*: Intestinal microbiota mediates the susceptibility to polymicrobial sepsis-induced liver injury by granisetron generation in mice. Hepatology 69: 1751-1767, 2019.
22. Liang H, Song H, Zhang X, Song G, Wang Y, Ding X, Duan X, Li L, Sun T and Kan Q: Metformin attenuated sepsis-related liver injury by modulating gut microbiota. Emerg Microbes Infect 11: 815-828, 2022.
23. Livak KJ and Schmittgen TD: Analysis of relative gene expression data using real-time quantitative PCR and the 2(-Delta Delta C(T)) method. Methods 25: 402-408, 2001.
24. Zhong X, Xiao Q, Liu Z, Wang W, Lai CH, Yang W, Yue P, Ye Q and Xiao J: TAK242 suppresses the TLR4 signaling pathway and ameliorates DCD liver IRI in rats. Mol Med Rep 20: 2101-2110, 2019.
25. Li S, Han S, Jin K, Yu T, Chen H, Zhou X, Tan Z and Zhang G: SOCS2 suppresses inflammation and apoptosis during NASH progression through limiting NF-κB activation in macrophages. Int J Biol Sci 17: 4165-4175, 2021.
26. Posselt G, Schwarz H, Duschl A and Horejs-Hoeck J: Suppressor of cytokine signaling 2 is a feedback inhibitor of TLR-induced activation in human monocyte-derived dendritic cells. J Immunol 187: 2875-2884, 2011.
27. Baetz A, Frey M, Heeg K and Dalpke AH: Suppressor of cytokine signaling (SOCS) proteins indirectly regulate toll-like receptor signaling in innate immune cells. J Biol Chem 279: 54708-54715, 2004.
28. Yang J, Zeng P, Yang J and Fan ZX: The role of RP105 in cardiovascular disease through regulating TLR4 and PI3K signaling pathways. Curr Med Sci 39: 185-189, 2019.
29. Divanovic S, Trompette A, Petiniot LK, Allen JL, Flick LM, Belkaid Y, Madan R, Haky JJ and Karp CL: Regulation of TLR4 signaling and the host interface with pathogens and danger: The role of RP105. J Leukoc Biol 82: 265-271, 2007.
30. Singer M, Deutschman CS, Seymour CW, Shankar-Hari M, Annane D, Bauer M, Bellomo R, Bernard GR, Chiche JD, Coopersmith CM, *et al*: The third international consensus definitions for sepsis and septic shock (sepsis-3). JAMA 315: 801-810, 2016.
31. Cecconi M, Evans L, Levy M and Rhodes A: Sepsis and septic shock. Lancet 392: 75-87, 2018.
32. Recknagel P, Gonnert FA, Westermann M, Lambeck S, Lupp A, Rudiger A, Dyson A, Carré JE, Kortgen A, Krafft C, *et al*: Liver dysfunction and phosphatidylinositol-3-kinase signalling in early sepsis: Experimental studies in rodent models of peritonitis. PLoS Med 9: e1001338, 2012.
33. Bastarache JA and Matthay MA: Cecal ligation model of sepsis in mice: New insights. Crit Care Med 41: 356-357, 2013.
34. Dejager L, Pinheiro I, Dejonckheere E and Libert C: Cecal ligation and puncture: The gold standard model for polymicrobial sepsis? Trends Microbiol 19: 198-208, 2011.
35. Rittirsch D, Huber-Lang MS, Flierl MA and Ward PA: Immunodesign of experimental sepsis by cecal ligation and puncture. Nat Protoc 4: 31-36, 2009.
36. Miyake K, Yamashita Y, Hitoshi Y, Takatsu K and Kimoto M: Murine B cell proliferation and protection from apoptosis with an antibody against a 105-kD molecule: Unresponsiveness of X-linked immunodeficient B cells. J Exp Med 180: 1217-1224, 1994.
37. Miura Y, Shimazu R, Miyake K, Akashi S, Ogata H, Yamashita Y, Narisawa Y and Kimoto M: RP105 is associated with MD-1 and transmits an activation signal in human B cells. Blood 92: 2815-2822, 1998.
38. Ishii A, Matsuo A, Sawa H, Tsujita T, Shida K, Matsumoto M and Seya T: Lamprey TLRs with properties distinct from those of the variable lymphocyte receptors. J Immunol 178: 397-406, 2007.
39. Yang J, Zhai Y, Huang C, Xiang Z, Liu H, Wu J, Huang Y, Liu L, Li W, Wang W, *et al*: RP105 attenuates ischemia/reperfusion-induced oxidative stress in the myocardium via activation of the Lyn/Syk/STAT3 signaling pathway. Inflammation 47: 1371-1385, 2024.
40. Guo X, Hu S, Liu JJ, Huang L, Zhong P, Fan ZX, Ye P and Chen MH: Piperine protects against pyroptosis in myocardial ischaemia/reperfusion injury by regulating the miR-383/RP105/AKT signalling pathway. J Cell Mol Med 25: 244-258, 2021.

41. Guo X, Jiang H and Chen J: RP105-PI3K-Akt axis: A potential therapeutic approach for ameliorating myocardial ischemia/reperfusion injury. Int J Cardiol 206: 95-96, 2016.
42. Liu B, Zhang N, Liu Z, Fu Y, Feng S, Wang S, Cao Y, Li D, Liang D, Li F, *et al*: RP105 involved in activation of mouse macrophages via TLR2 and TLR4 signaling. Mol Cell Biochem 378: 183-193, 2013.
43. Huang W, Yang J, He C and Yang J: RP105 plays a cardioprotective role in myocardial ischemia reperfusion injury by regulating the Toll-like receptor 2/4 signaling pathways. Mol Med Rep 22: 1373-1381, 2020.
44. Sun Y, Liu L, Yuan J, Sun Q, Wang N and Wang Y: RP105 protects PC12 cells from oxygen-glucose deprivation/reoxygenation injury via activation of the PI3K/AKT signaling pathway. Int J Mol Med 41: 3081-3089, 2018.
45. Sarajlic M, Neuper T, Föhrenbach Quiroz KT, Michelini S, Vetter J, Schaller S and Horejs-Hoeck J: IL-1β induces SOCS2 expression in human dendritic cells. Int J Mol Sci 20: 5931, 2019.
46. Krebs DL and Hilton DJ: SOCS proteins: Negative regulators of cytokine signaling. Stem Cells 19: 378-387, 2001.
47. Elliott J and Johnston JA: SOCS: Role in inflammation, allergy and homeostasis. Trends Immunol 25: 434-440, 2004.
48. Keating N and Nicholson SE: SOCS-mediated immunomodulation of natural killer cells. Cytokine 118: 64-70, 2019.
49. Hu J, Winqvist O, Flores-Morales A, Wikström AC and Norstedt G: SOCS2 influences LPS induced human monocyte-derived dendritic cell maturation. PLoS One 4: e7178, 2009.
50. Zhang D, Pan A, Gu J, Liao R, Chen X and Xu Z: Upregulation of miR-144-3p alleviates Doxorubicin-induced heart failure and cardiomyocytes apoptosis via SOCS2/PI3K/AKT axis. Chem Biol Drug Des 101: 24-39, 2023.
51. Monti-Rocha R, Cramer A, Gaio Leite P, Antunes MM, Pereira RVS, Barroso A, Queiroz-Junior CM, David BA, Teixeira MM, Menezes GB and Machado FS: SOCS2 is critical for the balancing of immune response and oxidate stress protecting against acetaminophen-induced acute liver injury. Front Immunol 9: 3134, 2018.